Title

Bone marrow changes related to disuse

Journal

European Radiology, 23(12)

ISSN

0938-7994

Authors

Nardo, Lorenzo

Sandman, David N

Virayavanich, Warapat

et al.

Publication Date

2013-12-01

DOI

10.1007/s00330-013-2943-6

Peer reviewed

Published in final edited form as:
Eur Radiol. 2013 December ; 23(12): 3422–3431. doi:10.1007/s00330-013-2943-6.

Bone Marrow Changes related to Disuse

Lorenzo Nardo, MD[1], **David N. Sandman, MD**[1], **Warapat Virayavanich, MD**[1], **Linlin Zhang, MS**[2], **Richard Souza, PhD**[1], **Lynne Steinbach, MD**[1], **Michele Guindani, PhD**[3], and **Thomas M. Link, MD, PhD**[1]

[1]Musculoskeletal and Quantitative Imaging Group (MQIR), Department of Radiology, University of California San Francisco, San Francisco, CA, USA

[2]Department of Statistics, Rice University, Houston, TX, USA

[3]Department of Biostatistics, University of Texas M.D. Anderson Cancer Center, Houston, TX, USA

Abstract

Objective—To evaluate bone marrow changes on knee MRI in patients with 3-to-6 week long period of unloading.

Materials and Methods—MRI knee examinations were performed in 30 patients (14 men, 16 women, aged 20–53 years) at baseline and 5–10 weeks after immobilization of the ipsilateral lower extremity; subsets of patients were examined at additional time points. Ten volunteers (4 men, 6 women; aged 20–50) were studied as control cohort at 2 time points. Bone marrow signal abnormalities were analyzed according to 1) severity, 2) signal alteration relative to hyaline cartilage, 3) morphology, 4) increased vascularity in the knee joint and 5) T1-signal alteration. Spearman rank correlation test (SRC) and Kendall's tau (KT) were used to compare individual scores.

Results—All 30 patients presented abnormal bone marrow findings after unloading, which reached a peak at 10–25 weeks (P <0.001). These findings decreased within one year (P <0.001). High scores of severity were associated with confluent and patchy patterns of bone marrow (SCR=0.923, P <0.01 and KT= 0.877 P <0.01).

Conclusion—Signal abnormalities of the bone marrow related to unloading are consistent findings and most prominent 10–25 weeks following immobilization when both confluent and patchy hyperintense patterns are present.

Keywords

Disuse; Magnetic Resonance Imaging; Knee; Findings; Bone Marrow

Corresponding author address: Lorenzo Nardo, MD, Department of Radiology and Biomedical Imaging, University of California, San Francisco, 185 Berry Street, Suite 350, San Francisco, CA, 94107, Lorenzo.Nardo@ucsf.edu, Tel: (415) 353-4928, Fax: (415) 353-1796.

Introduction

Disuse osteopenia results from reduced weight-bearing on lower limbs, leading to loss of bone mass, compromised bone architecture, and increased fracture rates [1–5]. The exact pathophysiological process of disuse is unknown. However, studies indicate bone resorption rather than decreases in bone formation [6–10]. Many factors play important roles in its pathogenesis such as changes in osteoprogenitor cell populations, sympathetic nervous system and interstitial fluid pressure [6; 7; 11]. Studies suggest that early remobilization or pharmaceutical interventions may prevent disuse [12; 13]. Therefore, recognizing the stages of disease is important.

The radiographic appearance of disuse has been established [14; 15] and few investigations have described the onset of disuse 4–8 weeks after immobilization [5; 6; 8; 16–18]. The greater sensitivity of MRI to marrow pathology would help with early diagnosis and monitoring treatment, potentially reducing morbidity associated with disuse [12; 13; 19] Few studies have reported bone abnormalities due to disuse: de Abreu [20] described disuse as large lobular regions of fat predominantly in the subarticular region of bone, scattered between accentuated coarsened trabecular bone and vertical trabecular lines. Fluid sensitive sequences with fat suppression show accentuation of bone vessels and diffusely multiple-dotted high signal changes throughout the involved bone [20; 21]. A study from Elias at al. [21] described similar findings: a specific subchondral and subcortical bone marrow oedema signal pattern characterized the ankle after a non weight-bearing period but the authors proposed a different etiology and described the MRI findings as unclear. They believed that not only disuse demineralization or regional migratory osteoporosis after immobilization of an extremity is responsible for the bone marrow oedema but also a physiologic stress response in involved bones, after resumption of weight-bearing activity.

Given the limited knowledge of disuse related bone marrow changes including their aetiology and development in MR studies, we aimed (i) to investigate and characterize morphology of bone marrow pattern in disuse, and (ii) to longitudinally evaluate bone marrow changes on MRI related to disuse in patients with lower extremity unloading (due to trauma or surgery) and early remobilization.

Materials and Methods

Patient cohort

This retrospective study complied with standards set forth by the Health Insurance Portability and Accountability Act (HIPAA) and was approved by the Committee for Human Research (CHR). We included subjects from previous studies analyzing unloading in 30 patients with ankle fractures (n=2), foot surgery (n=10) and ACL reconstruction (n=18). Surgery was performed after 2 to 4 weeks for ACL injury and within a week for ankle fractures. Foot surgery was performed for deformities that resulted in problems with ambulation, such as hallux valgus. Inclusion criteria consisted of (i) non-weight-bearing of the ipsilateral lower extremity for 3 to 6 weeks, (ii) MR imaging within two weeks from onset of immobilization, and (iii) at least one follow-up MRI exam 5–10 weeks from onset of immobilization. Follow-up examinations were included if separated by at least a four-

week interval. Exclusion criteria consisted of (i) metallic hardware in the knee obscuring evaluation of bone marrow, (ii) lack of sagittal fat-saturated intermediate weighted FSE sequence in the protocol and (iii) incomplete clinical data regarding timeline of immobilization. Using these criteria, 30 patients (14 men, 16 women) with a mean age of 33.9 years (men age range, 20–49 years; women age range, 22–53 years) had at least two MRIs obtained after injury (one within two weeks and one after 5–10 weeks from onset of immobilization). 30 subjects had two MRIs, 25 subjects had three, 16 subjects had four, and 11 had five MRIs after immobilization. The MRI obtained within 2 weeks was defined as the baseline MRI, the first follow-up occurred 5–10 weeks from the onset of immobilization, the second after 10–25 weeks, the third after 25–65 weeks and the fourth after a period longer than 65 weeks from the onset of immobilization. Fig. 1 shows the relationship between MRI studies and weight bearing/non-weight bearing period.

Control cohort

The control cohort consisted of subjects from a study assessing the impact of running on cartilage (18); those subjects were imaged with the same sequences as the patient cohort. Inclusion criteria consisted of (i) no history of immobilization or knee-injury (ii) at least 2 MRI studies acquired 3 months apart. The 10 subjects were matched with the patient cohort based on age and sex (4 men, 6 women; mean age, 30 years; age range: for men, 20–46 years; for women, 22–50 years).

MR imaging and image analysis

Knee MR examinations were performed with a 3.0-T scanner (MR750; GE Healthcare, Milwaukee, USA) with an 8-channel knee surface coil (GE Healthcare, Milwaukee, USA). MRI sequence selection is presented in Table 1.

Studies were reviewed using PACS workstations (Agfa, Ridgefield Park, USA). As a “training period”, three musculoskeletal radiologists (**BLINDED**) analyzed 48 MRI studies (obtained in 15 patients) to obtain a consensus reading and calibrate grading disuse pattern. MRI studies were reviewed independently by two radiologists blinded by the different cohorts. In instances where scores were different, the third MSK radiology performed consensus readings.

Each knee was divided into 3 compartments: patella, tibia and femur; the patella was subdivided into intracortical, subcortical, intramedullary and subchondral compartments; the tibial and femoral diaphysis and metaphysis were divided into intracortical, subcortical and intramedullary compartments; the tibial and femoral epiphysis were divided into subchondral and intramedullary compartments.

Altogether, 20 subregions were identified and graded as shown in Table 2 for the following morphological criteria as seen on fluid sensitive fat-saturated images: (i) bone marrow signal abnormality (none, subtle—10% of subregion, mild—10–40% of subregion, moderate—> 40% of subregion or severe-> 75% of subregion); (ii) signal intensity relative to hyaline cartilage (hypointense, isointense, hyperintense); (iii) morphology of signal alteration (no present, dotted, linear, patchy or confluent); (iv) presence or absence of hypervascularity [2, 9, 16], qualitatively defined as increased serpiginous linear vascular structures in the

periphery of the bone [2, 9]; (v) presence of alteration on T1-weighted images recorded as present or absent. Fig. 3 shows examples for different morphological criteria and grades of abnormalities.

Statistical Analysis

Chi-square tests were used to compare differences in assessed parameters of each bone subregion and also between genders, between age groups, between disease and control groups, and between ACL and fracture patients at time point 2. Fisher's exact tests were used to confirm small cell counts of the corresponding contingency table. Spearman rank correlation tests were used to analyze the correlation between bone marrow signal abnormalities, signal intensity relative to cartilage, morphology and hypervascularity.

McNemar's tests were used to study statistically significant changes in scores of bone marrow signal abnormality, signal intensity relative to hyaline cartilage, morphology, and hypervascularity as seen on fluid sensitive fat-saturated images across follow-ups. Significance was set as 0.05 for all calculations unless otherwise stated. The *P*-values were adjusted for multiplicity using the Holm-Bonferroni correction, which controls the family-wise error rate. Statistical analysis was performed with R software version 2.14.2 for Windows.

Reproducibility Analyses

Inter-observer reproducibility measurements were obtained using all the MRI studies (image review was performed independently by 2 radiologists). Intra-observer reproducibility measurements were obtained using 50 randomly selected MRI studies. Two radiologists (**BLINDED**) independently analyzed each image set on two separate occasions. Cohen's Kappa values were calculated to assess intraobserver and interobserver agreement of the disuse score system classification.

Results

Characterization of Findings

Bone marrow changes were most conspicuous at time point 2, which contained MRIs of 25 subjects analyzed as follows:

Location of signal abnormalities within the knee—Signal abnormalities related to disuse were mostly found in the patella and femur 24/25 subjects (96%) (Fig. 4). The tibia was involved in 21/25 subjects (84%). In 3 subjects the findings involved only two bones: femur and patella. The patella demonstrated higher 'extent' scores when compared with femur or tibia (P <0.001) and the femur demonstrated higher 'extent' scores when compared with the tibia (P =0.019). Within the patella, no differences in 'extent' scores were found amongst subcompartments. Within the femur, the epiphyseal intramedullary, the epiphyseal subchondral and the metaphyseal intracortical sub-compartments were the most severely affected (P <0.001) and within the tibia, the subchondral subcompartment was the most affected (P <0.001). The diaphysis was never involved by signal changes associated with disuse.

High ‘extent’ scores correlated with hypervascularity (Spearman rank correlation coefficient 0.540; Kendall rank correlation coefficient 0.491; P <0.001), ‘patchy’ or ‘confluent’ morphology patterns (Spearman rank correlation coefficient 0.923; Kendall rank correlation coefficient 0.877; P <0.001) and hyperintensity relative to hyaline cartilage on fluid sensitive images (Spearman rank correlation coefficient 0.645; Kendall rank correlation coefficient 0.594; P <0.001). The ‘patchy’ or ‘confluent’ morphology patterns were associated with hypervascularity (Spearman rank correlation coefficient 0.622; Kendall rank correlation coefficient 0.564; P < 0.001). Hyperintensity was associated with hypervascularity (Spearman rank correlation coefficient was 0.362, Kendall rank correlation coefficient 0.347; P < 0.001).

Controls did not show any signal abnormalities consistent with disuse.

Longitudinal Evaluation of Bone Marrow Changes

At baseline none of the 30 patients had bone marrow abnormalities observed with disuse. At follow-up one (5–10 weeks), all patients developed signal abnormalities (increased vascularity and/or severity score equal to or greater than 1). Fig. 5 illustrates disuse related findings over a 32-week period. No significant differences in DO-related MR findings were observed by sex or age.

Extent of bone marrow signal abnormality—Hyperintensity within the bone marrow was greatest at follow-up two with a statistically significant increase compared to follow-up one (P values ranged from 0.008 to 0.015 after multiple adjustments in the femoral compartment). A representative image is shown in Fig. 6. At follow-up two, twelve subjects (48%) had an extent score equal or larger than 3 (bone marrow changes > 40% of the subregion) in at least one subcompartment. There was a statistically significant decrease in extent of signal abnormality on follow-up three relative to follow-up one and two (P values range from 0.023 to 0.041). No statistically significant differences were found between follow-up three and four, three and baseline, and four and baseline. In none of the eleven subjects with a follow-up longer than 65 weeks bone marrow abnormalities related to disuse were found.

Morphology—Patchy and confluent patterns of signal abnormalities were more frequently at follow-up two compared to follow-up one, where the linear and dot patterns predominated; this difference was statistically significant (P values ranged from 0.001 to 0.013 in different subcompartments). At follow-up two, 16/25 (64%) subjects presented signal abnormality characterized by a patchy or patchy and confluent pattern in at least one subcompartment while at follow-up one, just one subject had a patchy distribution of bone marrow alteration and 29/30 patients had a dot-like or linear pattern of bone marrow alteration. At follow-up three the linear and dot-like patterns again predominated and the change compared to follow-up two was statistically significant (P values ranged from 0.005 to 0.027 in different subcompartments). No significant changes between follow-ups three and four were observed Fig. 7 shows a representative example of morphology pattern distribution.

Signal intensity of the bone marrow relative to hyaline cartilage—Signal abnormalities were more frequently hyperintense compared to hyaline cartilage at follow-up two than for follow-up one (P <0.001). The percentage of score 3 at follow-up two was significantly greater than that at follow-up one and three. The proportion of signal intensities hyperintense to cartilage decreased in follow-up three and four compared to follow-up two (P <0.001) and finally returned to baseline; a representative example is shown in Fig. 8.

Hypervascularity—24/30 (80%), 23/30 (77%) and 17/30 (57%) of subjects had findings consistent with serpiginous linear hypervascularity in the periphery of the bone at follow-up one for patella, femur and tibia, respectively. There was no significant difference between follow-up one and follow-up two, but a significant decrease in this pattern was noted between follow-up two and three (P <0.001). No differences were again observed between follow-ups three and four (Fig. 4). At follow-up four none of the eleven patients had signs of increased vascularity. A representative example is shown in Fig. 9.

T1 signal intensity alterations: no statistically significant differences were found with regard to T1 signal intensity alterations at any point of the study.

Comparison between cohorts and subcohorts

No difference in signal patterns was found when the ACL injury subcohort was compared to foot surgery and ankle fracture subjects: extent, morphology and signal intensity were assessed in each subcompartment and no significant changes were found.

None of the control subjects had findings of disuse; when the control cohort was compared to the patient cohort, there was a significant difference in scores for all parameters assessed (with the exception of T1 abnormalities): P values were <0.001 for severity, morphology, vascularity and signal intensity gradings.

Reproducibility Analyses

Inter-observer reproducibility measurements were obtained using all MRI studies (image review was performed independently by 2 radiologists). Intra-observer reproducibility measurements were obtained using 50 randomly selected MRI studies (between patients and controls). Two radiologists (**BLINDED**) independently analyzed each image set on two separate occasions. Cohen’s Kappa values were calculated to assess intraobserver and interobserver agreement of the disuse score system classification. The combined weighted Cohen’s kappa values for inter-observer and intra-observer reproducibility of the disuse scoring system (for all gradings and subregions) were 0.91 and 0.98, respectively. These findings suggest high reproducibility.

Discussion

Our study demonstrated that in all of the immobilized patients 5 to 10 weeks after injury, bone marrow signal abnormalities consistent with disuse osteopenia were found, worsening over the next 10–25 weeks. Thereafter, abnormalities slowly disappeared and showed a morphology similar to that found at baseline. The DO findings were more severe at the

patella than at the femur and at the femur more severe than at the tibia. High severity scores were associated with complex morphology pattern, with signal alteration values higher than that of cartilage and increased vascularity.

Disuse osteopenia occurs as a result of prolonged inactivity or immobilization and is characterized by a decrease in bone mineral density [3; 14; 16; 17; 19]. A lot of studies have described the bone changing process beginning with the immobilization period [1; 3; 8; 14; 18; 22–24]. Most of these studies used blood and urine tests to assess the loss of calcium as well as radiological exams such as two dimensional dual-energy x-ray absorptiometry (DXA) and quantitative CT (QCT) techniques to evaluate the loss of bone. These studies demonstrated that bone change starts with the non-weighted bearing period and can be detected 4–6 weeks after the immobilization period (the entity is different according to individual parameters). In a study carried out using a cohort of patients with ankle fractures the peak of the bone loss was around 4 months; the timing for the peak has been discussed in the literature [2; 3; 5; 7; 11; 18], ranging between 4 to 10 weeks. The original bone mass will not be achieved for many years and the architecture of the bone will never been restored, resulting in weaker bone than normal [25] that is easier to break [26]. This metabolism of the bone can be shown using MRI technique. MRI images can depict both the subtle and advanced changing in the bone mass. In our work the first follow up was characterized by subtle dot like or linear morphology patterns with signal intensity higher than cartilage and associated with increased vascularity, evidence of the first metabolic change in the bone. The increased vascularity should be explained by the hyperemic state of the disused bone marrow [27]. The T2-abnormalities may reflect area of stress reaction the stress in the disused bone is bigger than in the normal bone because the trabeculae, which have to support the load, are less and weaker. The successively follow up demonstrated more severe findings associated with high prevalence of patchy and confluent morphology patterns having signal intensity higher than the cartilage, possibly, ascribable to the peak of the bone loss. Our series demonstrated that during follow-up 3 and 4, progressively the MRI findings became subtle or disappeared.

Not many works have been carried out with a longitudinal component, the most similar to our study was carried out by Elias et al. [21]. This work is different from ours because the authors have an immobilization period ranging between 4 and 18 weeks while ours is 3–6 weeks for all the subjects. All their patients showed disuse MRI finding within 12 weeks after the completion of the immobilization period and the findings did not progress after 18 weeks (after completion of the immobilization period). Although the different range of the immobilization period their results are similar to ours: all the patients who developed disuse had MRI-signs during the first and second follow up and those findings decreased/ disappeared during further follow ups.

Limitations of our study include the lack of any histological proof regarding the imaging findings we detected in our cohorts and the retrospective nature of the study. Also the term “disuse” may be a misnomer, particularly since bone marrow signal abnormalities are most prominent during the early weight-bearing period, the etiology of which is likely multifactorial as previously discussed and bone marrow abnormalities lack behind actual biomechanical loading. Moreover, it is not known whether microfractures related to a

weaker bone or a physiologic stress response may explain bone marrow abnormalities; this would need to be investigated in a dedicated study specifically focusing on the reloading phase.

In summary, this study has shown a spectrum of disuse related bone marrow abnormalities on MR imaging using fluid sensitive. These findings were most prominent 10–25 weeks following injury after early mobilization and associated with patchy or confluent morphologic patterns, T2 hyperintense signal relative to hyaline cartilage and covered more than 40% of bone subregions. They were most pronounced at the femur in the subchondral and intramedullary distal epiphysis, intracortical metaphysis and at the tibia in the subchondral subcomparment; furthermore these bone marrow alterations were often times associated with increased vascularity in the periphery of the bone.

Acknowledgments

Funding

NIH R01-AR057336

NIH P30-AR058899

References

1. Joyce JM, Keats TE. Disuse osteoporosis: mimic of neoplastic disease. Skeletal Radiol. 1986; 15:129–132. [PubMed: 3961518]
2. Luria T, Matsliah Y, Adir Y, et al. Effects of a prolonged submersion on bone strength and metabolism in young healthy submariners. Calcif Tissue Int. 2010; 86:8–13. [PubMed: 19882096]
3. Sievanen H. Immobilization and bone structure in humans. Arch Biochem Biophys. 2010; 503:146–152. [PubMed: 20637174]
4. Uebelhart D, Demiaux-Domenech B, Roth M, Chantraine A. Bone metabolism in spinal cord injured individuals and in others who have prolonged immobilization. A review. Paraplegia. 1995; 33:669–673. [PubMed: 8584303]
5. Uebelhart D, Hartmann D, Vuagnat H, Castanier M, Hachen HJ, Chantraine A. Early modifications of biochemical markers of bone metabolism in spinal cord injury patients. A preliminary study. Scand J Rehabil Med. 1994; 26:197–202. [PubMed: 7878394]
6. Lang TF, Leblanc AD, Evans HJ, Lu Y. Adaptation of the proximal femur to skeletal reloading after long-duration spaceflight. J Bone Miner Res. 2006; 21:1224–1230. [PubMed: 16869720]
7. Li XJ, Jee WS, Chow SY, Woodbury DM. Adaptation of cancellous bone to aging and immobilization in the rat: a single photon absorptiometry and histomorphometry study. Anat Rec. 1990; 227:12–24. [PubMed: 2195916]
8. Maimoun L, Couret I, Mariano-Goulart D, et al. Changes in osteoprotegerin/RANKL system, bone mineral density, and bone biochemicals markers in patients with recent spinal cord injury. Calcif Tissue Int. 2005; 76:404–411. [PubMed: 15812577]
9. Marchetti ME, Houde JP, Steinberg GG, Crane GK, Goss TP, Baran DT. Humeral bone density losses after shoulder surgery and immobilization. J Shoulder Elbow Surg. 1996; 5:471–476. [PubMed: 8981273]
10. Poole KE, Warburton EA, Reeve J. Rapid long-term bone loss following stroke in a man with osteoporosis and atherosclerosis. Osteoporos Int. 2005; 16:302–305. [PubMed: 15197547]
11. van der Meulen MC, Morgan TG, Yang X, et al. Cancellous bone adaptation to in vivo loading in a rabbit model. Bone. 2006; 38:871–877. [PubMed: 16431171]
12. Chappard D, Minaire P, Privat C, et al. Effects of tiludronate on bone loss in paraplegic patients. J Bone Miner Res. 1995; 10:112–118. [PubMed: 7747617]

13. Sholas MG, Tann B, Gaebler-Spira D. Oral bisphosphonates to treat disuse osteopenia in children with disabilities: a case series. J Pediatr Orthop. 2005; 25:326–331. [PubMed: 15832148]
14. Jones G. Radiological appearances of disuse osteoporosis. Clin Radiol. 1969; 20:345–353. [PubMed: 5349340]
15. Young DR, Schneider VS. Radiographic Evidence of Disuse Osteoporosis in the Monkey (M-Nemestrina). Calcified Tissue International. 1981; 33:631–639. [PubMed: 6799175]
16. Maimoun L, Fattal C, Sultan C. Bone remodeling and calcium homeostasis in patients with spinal cord injury: a review. Metabolism. 2011; 60:1655–1663. [PubMed: 21632079]
17. Shymkiw RC, Bray RC, Boyd SK, Kantzas A, Zernicke RF. Physiological and mechanical adaptation of periarticular cancellous bone after joint ligament injury. J Appl Physiol. 2001; 90:1083–1087. [PubMed: 11181623]
18. Tsubota K, Adachi T, Tomita Y. Functional adaptation of cancellous bone in human proximal femur predicted by trabecular surface remodeling simulation toward uniform stress state. J Biomech. 2002; 35:1541–1551. [PubMed: 12445607]
19. Lang TF. What do we know about fracture risk in long-duration spaceflight? J Musculoskelet Neuronal Interact. 2006; 6:319–321. [PubMed: 17185806]
20. de Abreu MR, Wesselly M, Chung CB, Resnick D. Bone marrow MR imaging findings in disuse osteoporosis. Skeletal Radiol. 2011; 40:571–575. [PubMed: 20953606]
21. Elias I, Zoga AC, Schweitzer ME, Ballehr L, Morrison WB, Raikin SM. A specific bone marrow edema around the foot and ankle following trauma and immobilization therapy: pattern description and potential clinical relevance. Foot Ankle Int. 2007; 28:463–471. [PubMed: 17475141]
22. Sugiyama T, Price JS, Lanyon LE. Functional adaptation to mechanical loading in both cortical and cancellous bone is controlled locally and is confined to the loaded bones. Bone. 2010; 46:314–321. [PubMed: 19733269]
23. Tandon SC, Gregson PA, Thomas PB, Saklatvala J, Singanayagam J, Jones PW. Reduction of post-traumatic osteoporosis after external fixation of tibial fractures. Injury. 1995; 26:459–462. [PubMed: 7493783]
24. Bloomfield SA. Disuse osteopenia. Curr Osteoporos Rep. 2010; 8:91–97. [PubMed: 20425616]
25. Browner, BDJJB.; Levine, AM.; Trafton, PG. Skeletal trauma. Saunders, editor. 2003. p. 3
26. Loomer PM. The impact of microgravity on bone metabolism in vitro and in vivo. Crit Rev Oral Biol Med. 2001; 12:252–261. [PubMed: 11497376]
27. Gross TS, Damji AA, Judex S, Bray RC, Zernicke RF. Bone hyperemia precedes disuseinduced intracortical bone resorption. J Appl Physiol. 1999; 86:230–235. [PubMed: 9887135]

Key Points

Disuse is associated with hyperintense MRI signal alteration on fluid sensitive sequence.

Disuse findings are more prominent at the patella and femoral epiphyses.

Disuse MRI findings appear characterized by a specific chronological pattern.

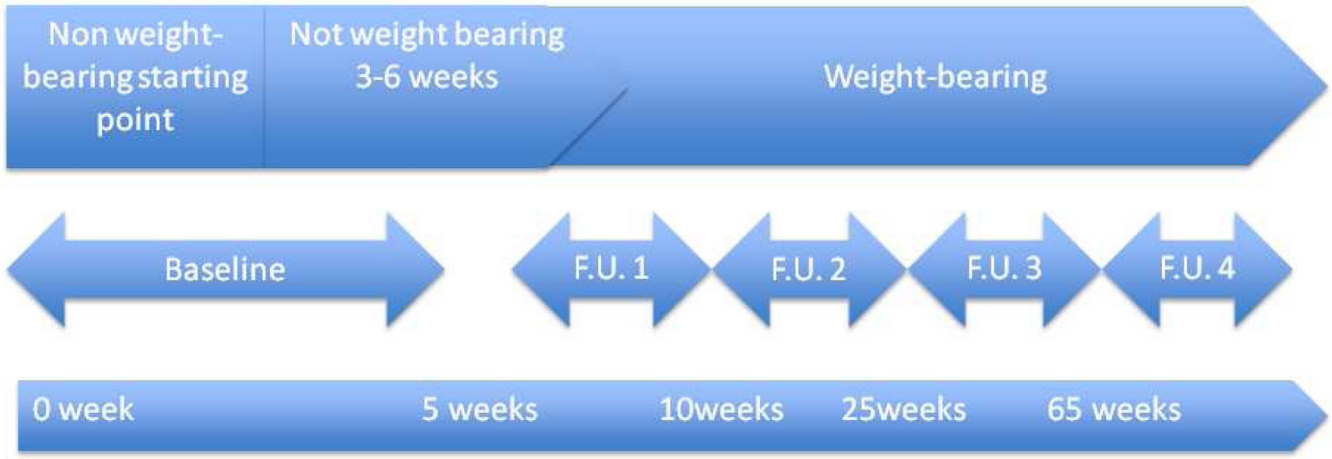

Fig. 1.

A diachronic picture of the time frames is seen in this Figure.; the MRI studies are aligneated with the time line (at the bottom; unit of measure weeks) and with the weight-bearing and not weight-bearing period (at the top). FU= follow-up

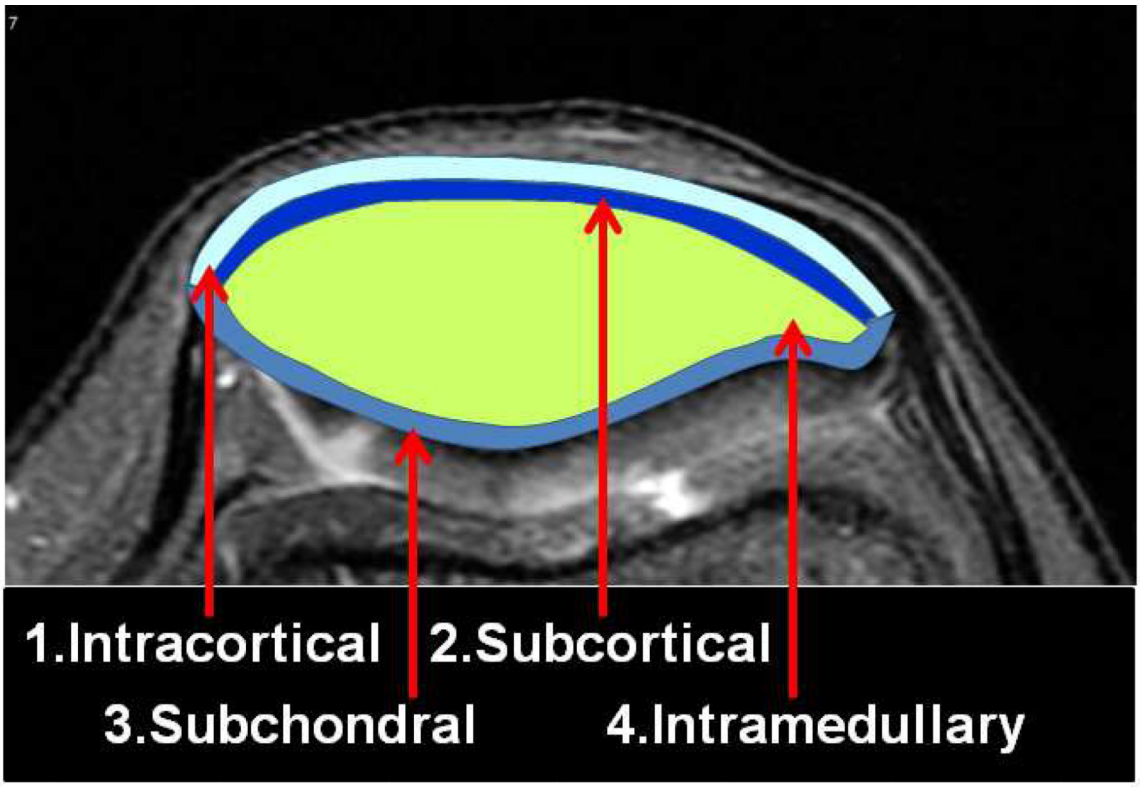

a

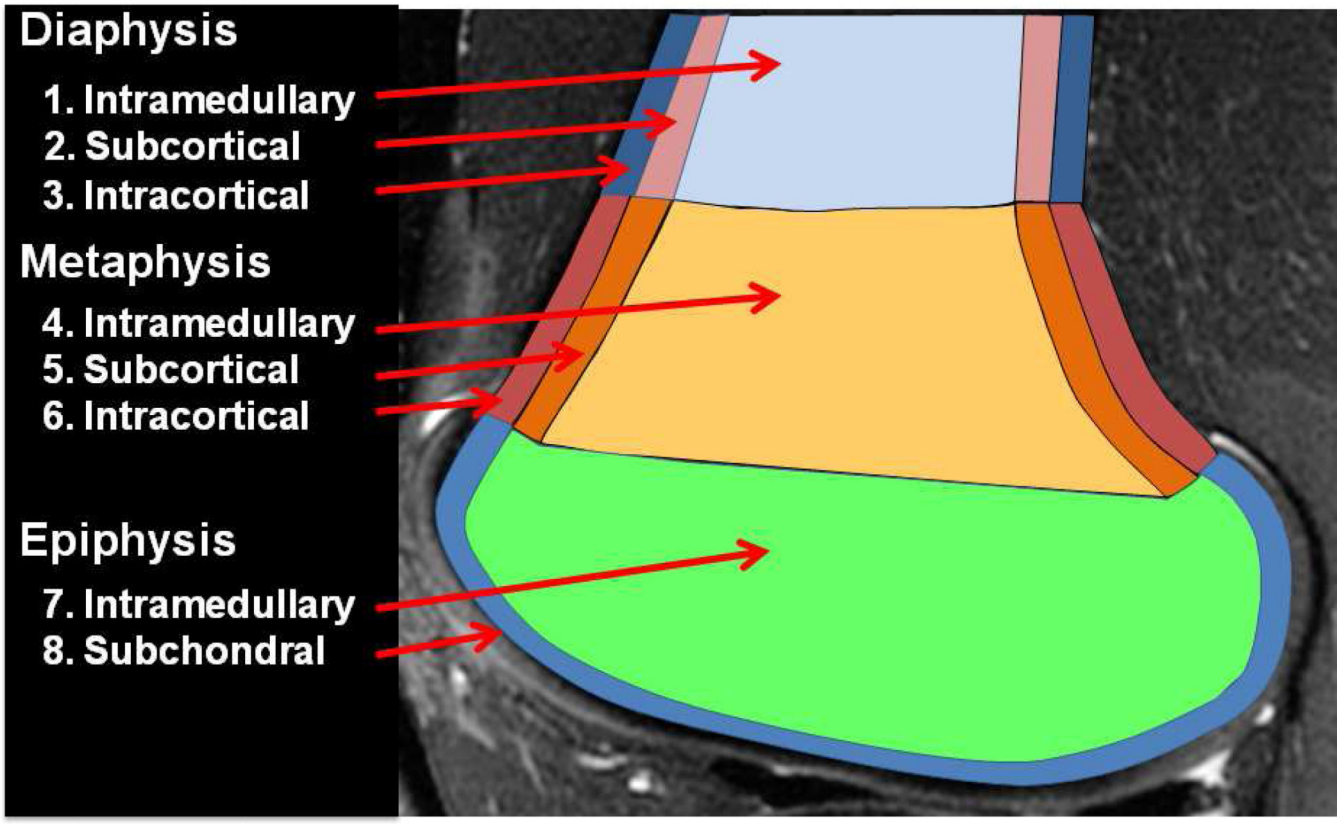

b

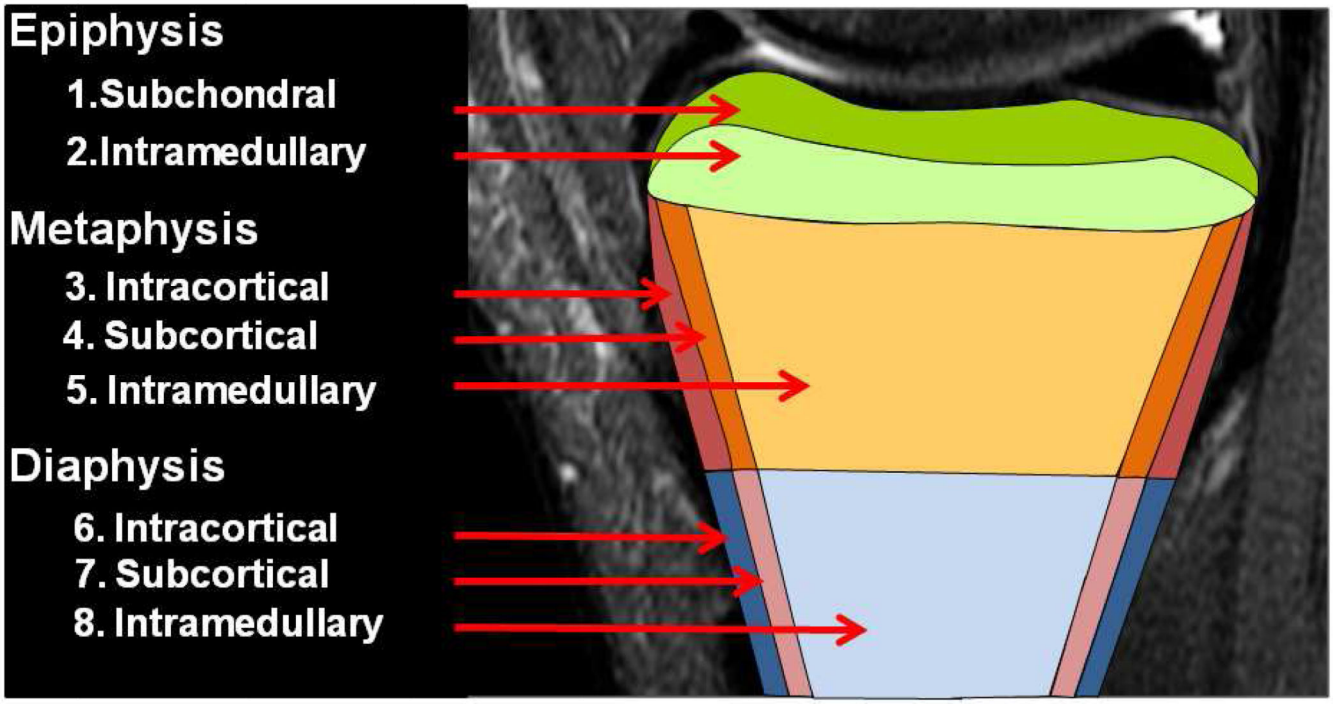

c

Fig. 2.

The studied subregions are illustrated.

a Four subregions at the patella: 1 intracortical, 2 subcortical, 3 subchondral, 4 intramedullary.

b Eight subregions at the femur: 1 diaphysis intramedullary, 2 diaphysis subcortical, 3 diaphysis intracortical, 4 metaphysis intramedullary, 5 metaphysis subcortical, 6 metaphysis intracortical, 7 epiphysis intramedullary, 8 epiphysis subchondral.

c Eight subregions at the tibia: 1 epiphysis subchondral, 2 epiphysis intramedullary, 3 metaphysis intracortical, 4 metaphysis subcortical, 5 metaphysis intramedullary, 6 diaphysis intracortical, 7 diaphysis subcortical, 8 diaphysis intramedullary

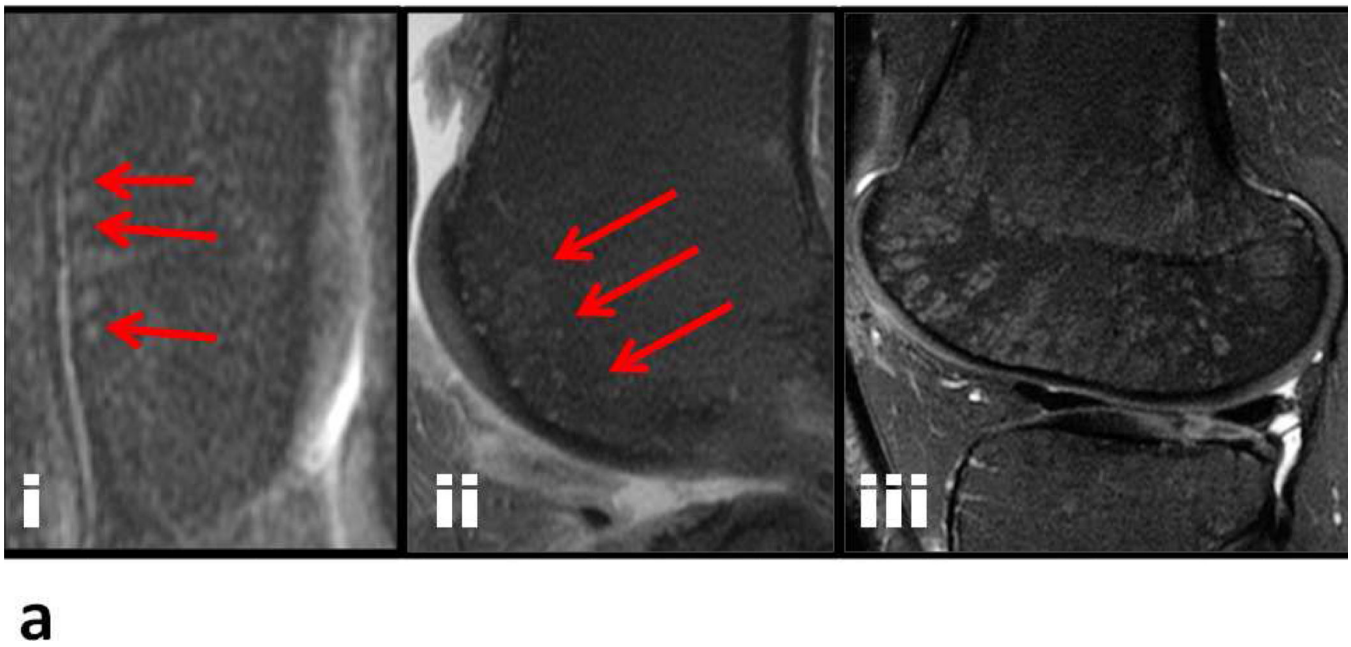

a

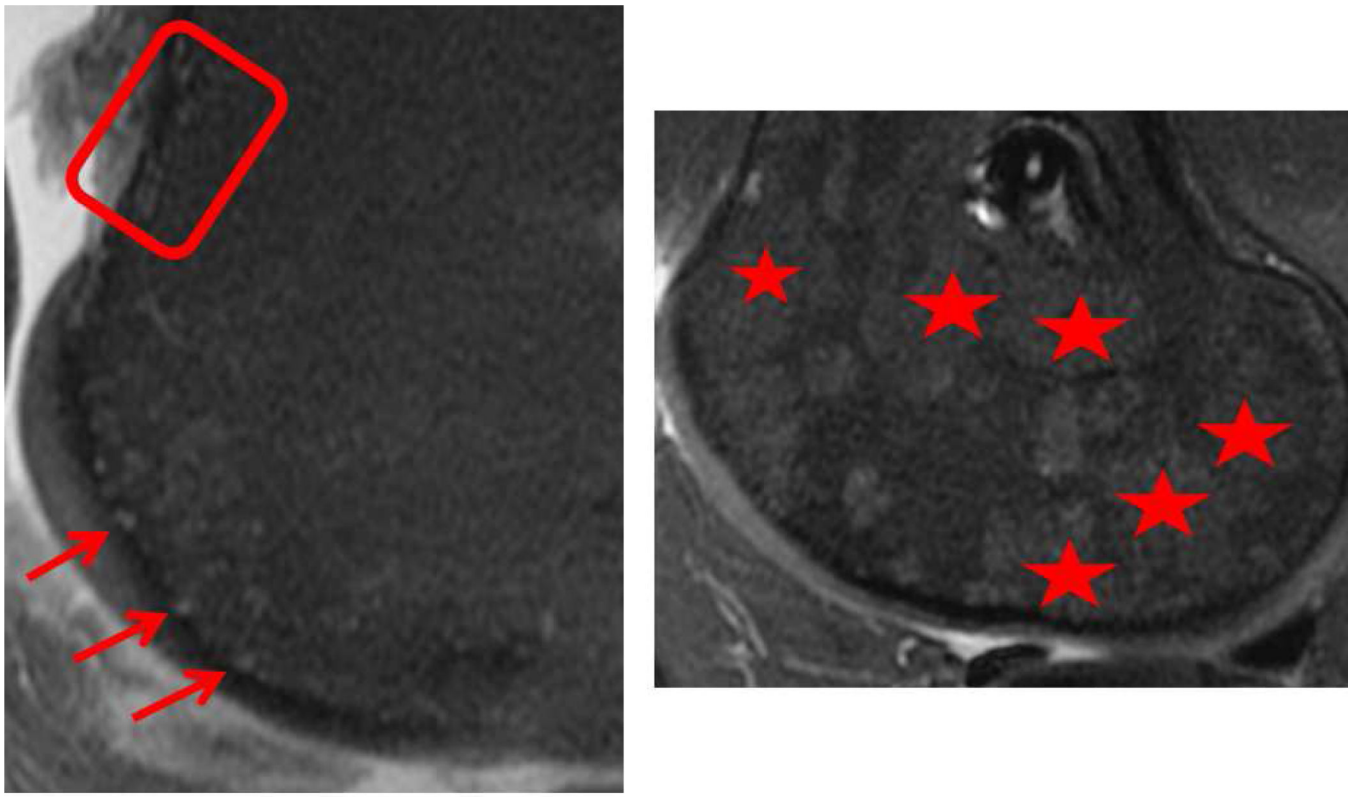

b

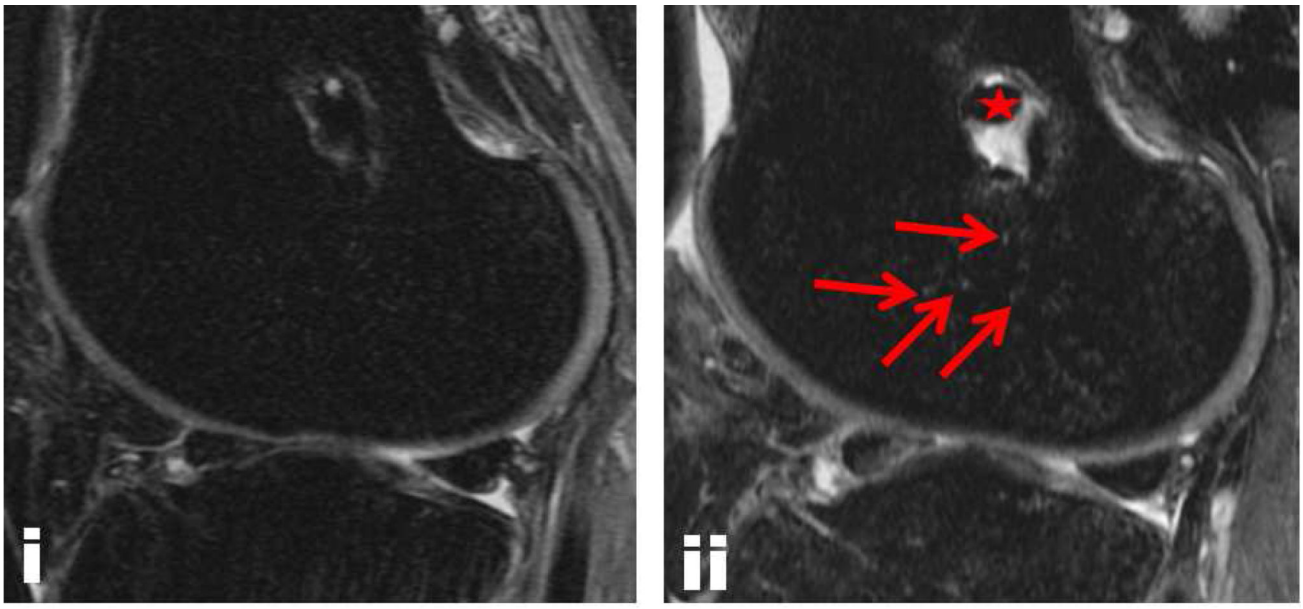

c

Fig. 3.

Representative sagittal fluid sensitive FSE images of the knee demonstrating different parameters and grades.

(a) The extent of the bone marrow abnormality was scored as mild (arrows) (i), moderate (arrows) (ii) and severe (iii).

(b) The morphology of the abnormality was scored as dot-like (arrows), linear (within the rectangle), patchy and confluent (stars).

(c) MR images in the same patient before (i) and after 6 weeks (ii) of immobilization. Increase in vascularity is well demonstrated. (The star indicates the ACL graft).

Fig. 4.

40 year-old male patient with ACL injury.

a) Sagittal fluid sensitive fat-suppressed MR image (TR= 4300 ms, TE= 50 ms) 6 days after injury, demonstrating normal red marrow (arrow) but otherwise no signal abnormalities.

b) Sagittal fluid sensitive fat-suppressed image (TR= 4300 ms, TE= 50 ms) 10 weeks after injury, demonstrating patchy alteration of signal (stars) in the epiphysis of the femur and in the patella subregions.

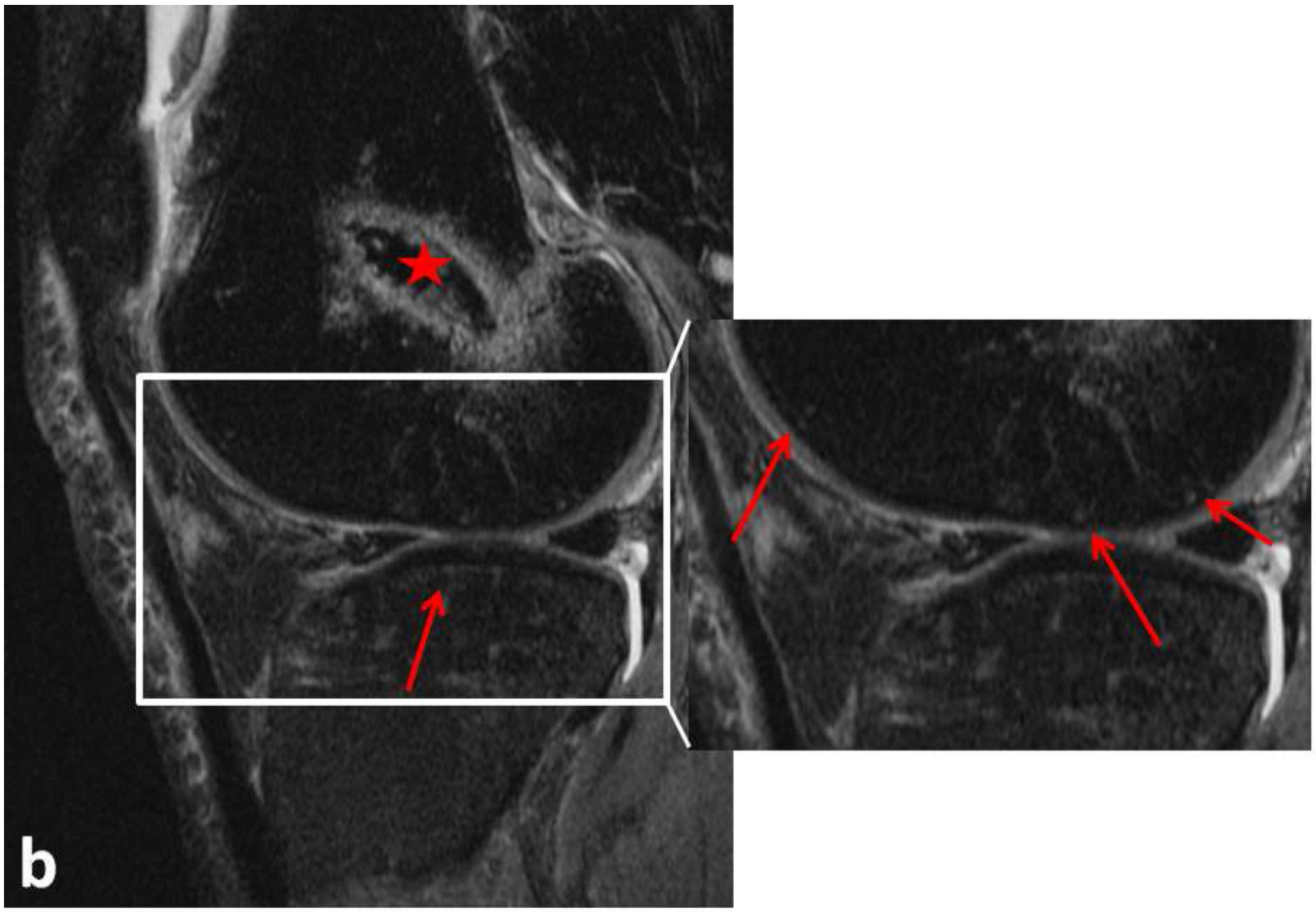

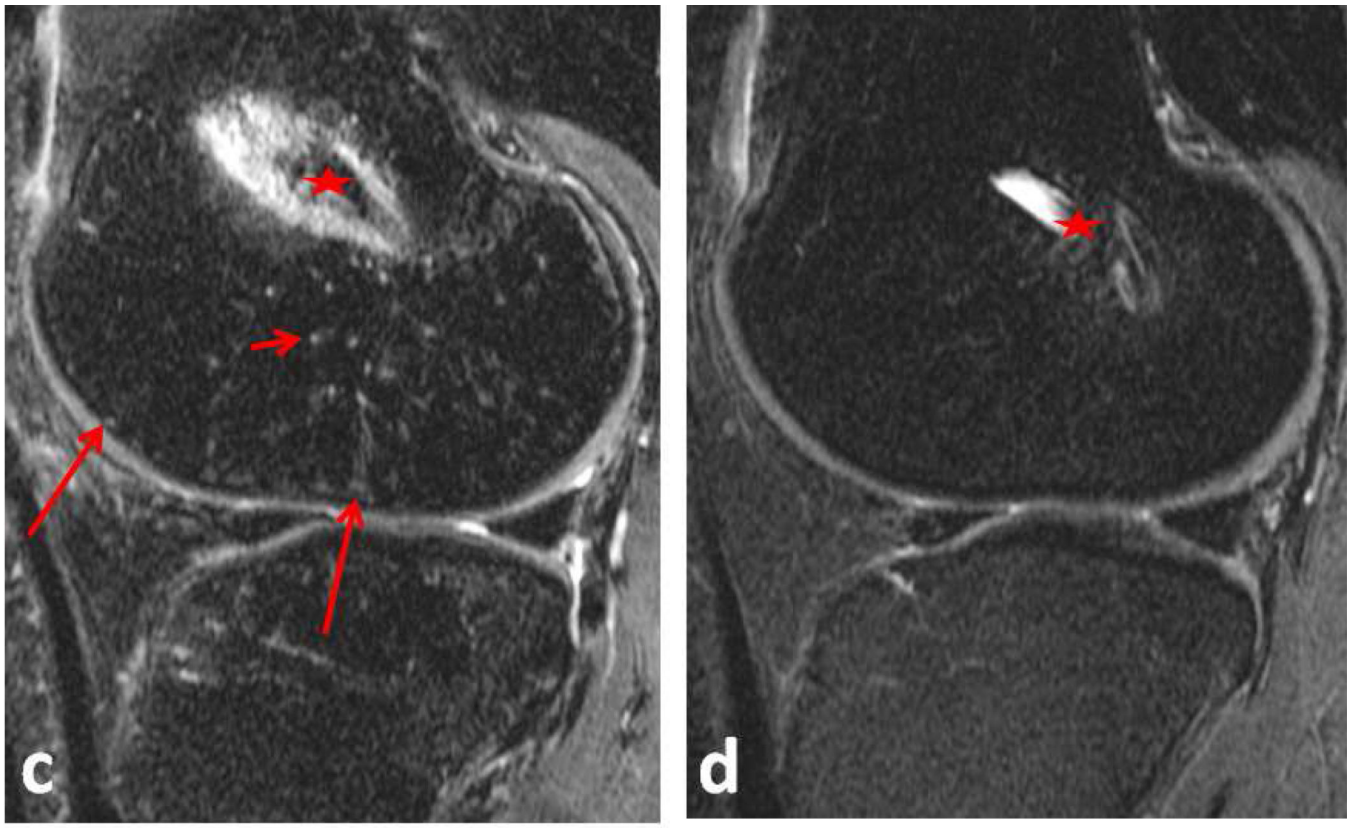

Fig. 5.

35 year-old woman suffering from ACL injury. The four sagittal fluid sensitive fat suppressed images (TR= 4300 ms TE= 50 ms) demonstrate the development of disuse from the baseline study through follow-up 4.

a) At the baseline study (1 week after injury), the fluid sensitive fat saturated sagittal MR image demonstrates the oedema pattern typical for ACL injury at the posterior aspect of the lateral tibial plateau (short arrow) and moderate supra-patellar joint effusion (long arrow). No signs of disuse are visible.

b) At the first follow-up (8 weeks after ACL reconstruction indicated by the star), the sagittal image demonstrates subtle onset of disuse; the arrows show dot-like signal alteration in the subchondral compartment of both tibia and femur.

c) At the second follow-up (16 weeks after ACL reconstruction, indicated by the star), the sagittal image demonstrates more severe bone marrow findings related to disuse: subchondral and intramedullary alterations of signal with dot like or linear morphology as indicated by long arrows. The short arrow indicates a prominent vessel.

d) At the third follow-up (32 weeks after ACL reconstruction, indicated by the star), no findings consistent with disuse are seen in the sagittal fluid sensitive fat saturated MR image.

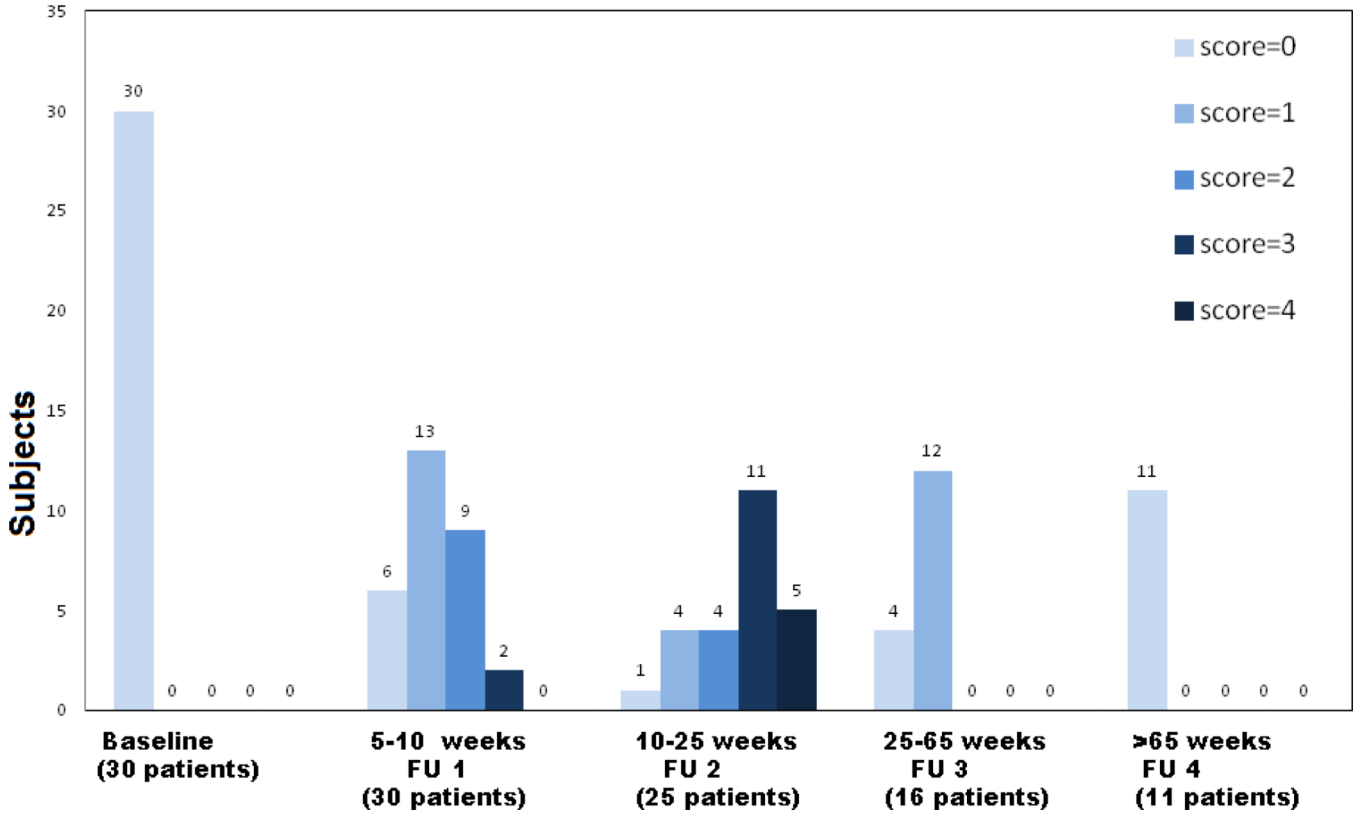

Fig. 6.

The semi-quantitative data for the extent of the bone marrow abnormalities are shown in the intramedullary femoral epiphyseal subregion over 5 time points: the largest number of patients with bone marrow signal abnormality and extent greater than 40% of the subregion is present at follow-up 2. Bone marrow signal abnormalities were not present at baseline and follow-up 4. (FU= follow up).

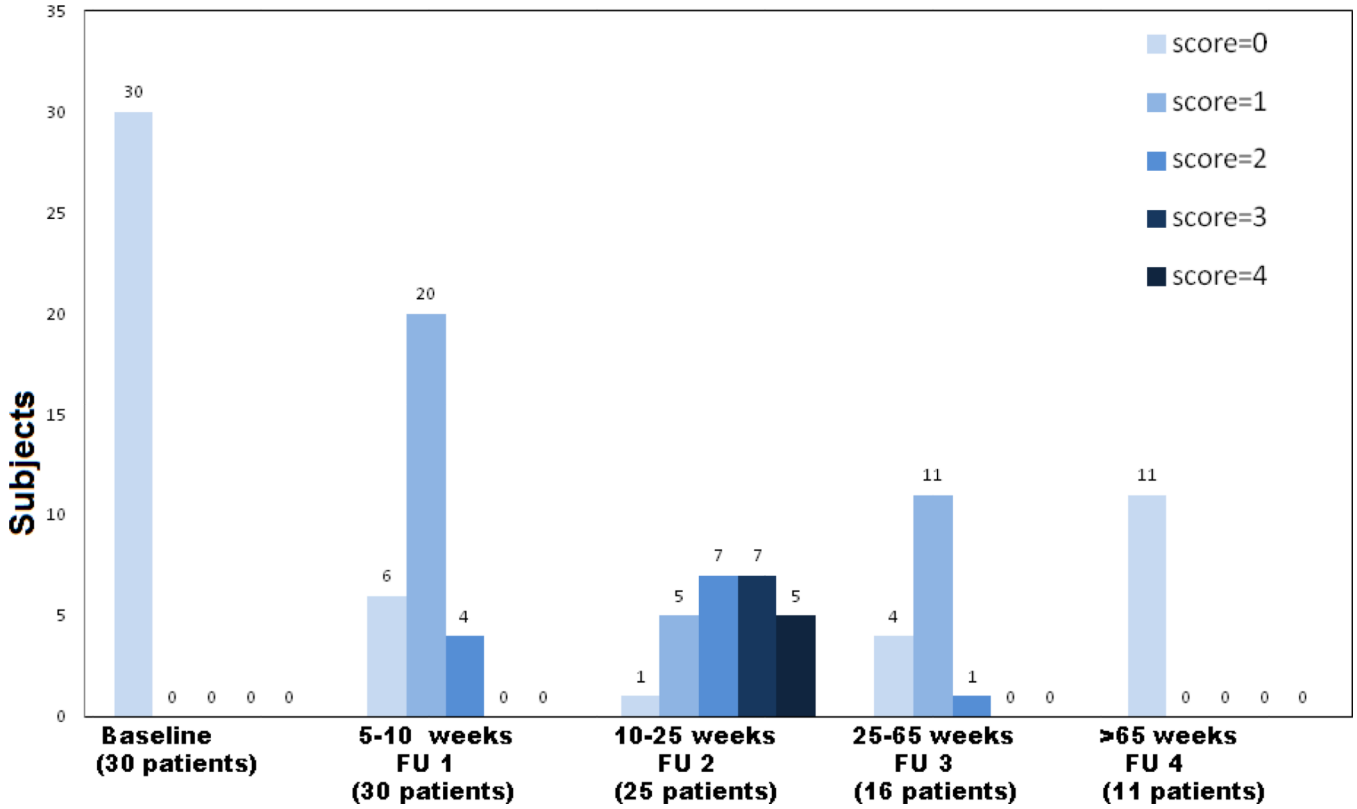

Fig. 7.

The semi-quantitative data for the morphology of the bone marrow abnormalities are shown in the intramedullary epiphysis of the femur epiphyseal subregion over 5 time points. At follow-up 2 the number of patients with patchy or patchy and confluent bone marrow oedema predominated. At follow-up 1 and 3 the dot-like pattern predominated. (FU= follow up)

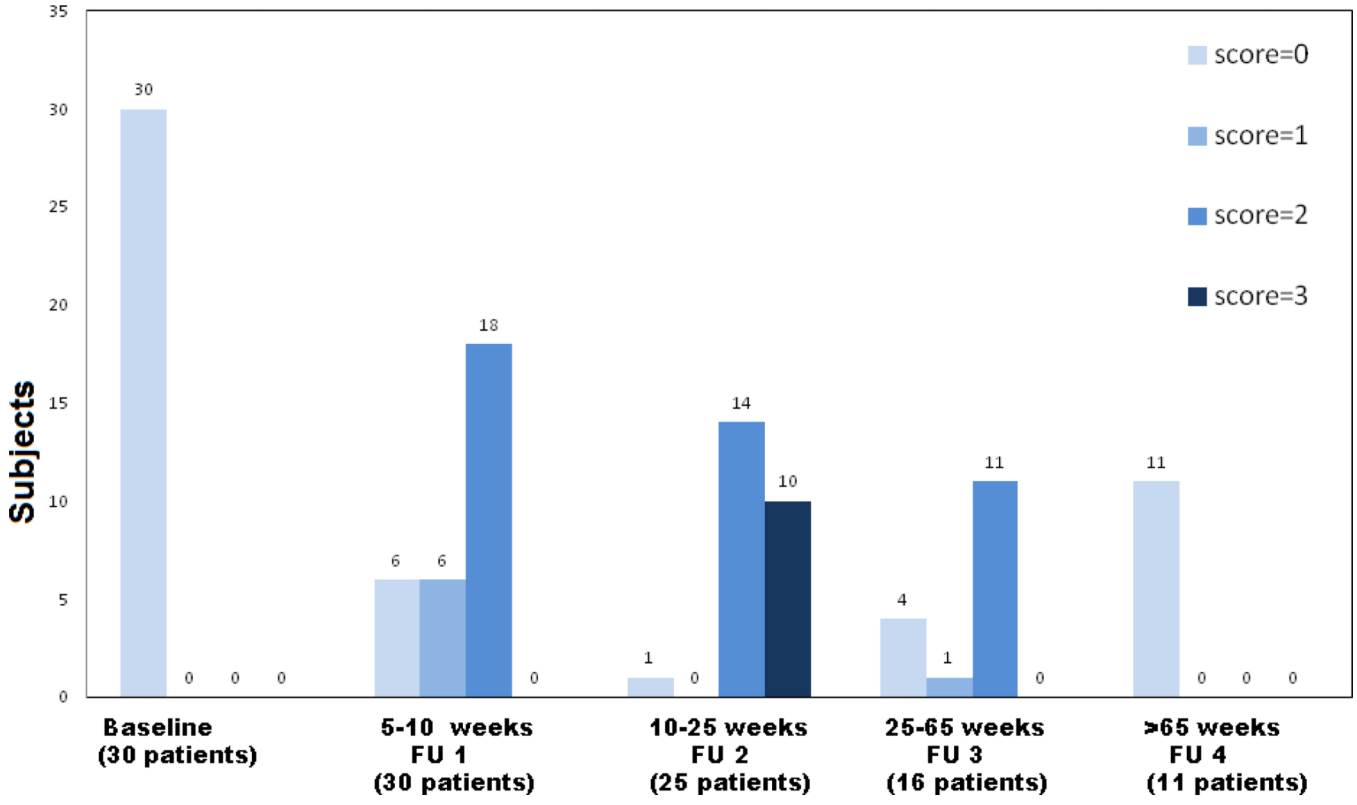

Fig. 8.

The semi-quantitative data for the signal intensity of the bone marrow abnormalities are shown in the intramedullary epiphysis of the femur epiphyseal subregion over 5 time points. At follow-up 2 the number of patients having bone marrow abnormalities with signal higher than the cartilage was significantly higher than at follow-up 1 and 3. (FU= follow up).

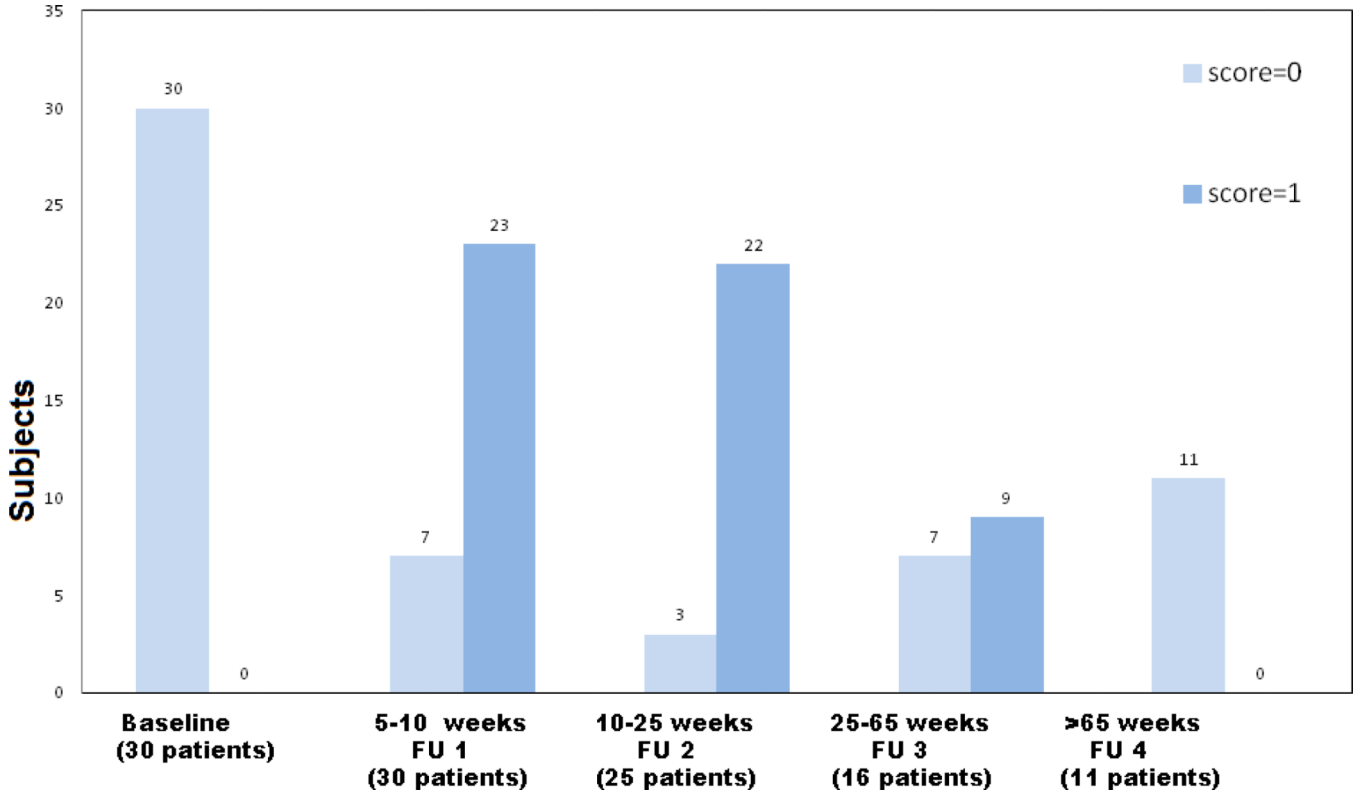

Fig. 9.

The semi-quantitative data for the increased vascularity is shown in the intramedullary epyphysis of the femur epiphyseal subregion over 5 time points. At follow-up 1 and 2 the number of patients with increased vascularity is significantly higher than at baseline and follow-up 3. (FU= follow up).

Table 1

Sequences acquired during the study with their individual parameters.

Sequence #	**1**	**2**	**3**	**4**
Sequence type	FSE intermediate-weighted, fat saturation	FSE intermediate-weighted, fat saturation	FSE T1	FSE intermediate-weighted, fat saturation
Plane	Sagittal	Axial	Coronal	Coronal
Field of view (cm)	13–16	13–16	13–16	13–16
Slice Thickness (mm)	2–4	4	4	4
TR in ms	4000	4000	500	4000
TE in ms	40	40	8	40

Table 2

Grading system. The analyzed parameters included (i) extent of bone abnormality, (ii) signal alteration relative to cartilage, (iii) morphological pattern, (iv) vascularity, v). Representative examples are shown in Fig. 3.

Parameter	Definition	Score
Extent of abnormality	Subtle (0–10%)	1
	Mild (10–40%)	2
	Moderate (40–75%)	3
	Severe (more than 75%)	4
Signal alteration*	Hypointense	1
	Isointense	2
	Hyperintense	3
Morphology	Dot-like	1
	Linear	2
	Patchy	3
	Patchy and confluent	4
Vascularity**	Normal	0
	Increased	1
Signal alteration on T1-W	Not present	0
	Present	1

*Relative to hyaline cartilage

**Qualitatively defined as increased serpiginous linear vascular structures in the subchondral or intracortical subregions of the peripheral bone.